J Mater Sci: Mater Electron (2013) 24:2112–2115
DOI 10.1007/s10854-013-1066-9

Structural, dielectric and magnetic characterization of large scale template synthesized Gd doped $BiFeO_3$ nanowires

Sanjeev Kumar

Received: 29 October 2012 / Accepted: 9 January 2013 / Published online: 18 January 2013

Abstract Pure and 10 % Gd doped $BiFeO_3$ nanowires of 100-nm diameter have been synthesized by sol–gel template-assisted technique. Phase-dependent structural, dielectric and magnetic properties of pure and Gd doped $BiFeO_3$ nanowires have been investigated. X-ray diffraction study reveals that pure $BiFeO_3$ nanowires possess rhombohedral structure while 10 % Gd doped $BiFeO_3$ nanowires are orthorhombic in nature. Magnetic study confirms that the value of saturation magnetization, increased with structural change via doping of Gd in host $BiFeO_3$.

1 Introduction

Nanoscale multiferroic materials possessing smaller size and effective magneto-electric coupling, unlock exciting numerous ways for scheming future nano-electronic and spintronics devices [1, 2]. As per the demand of future technology, multifunctional oxide nanostructures can play an important role in fulfilling the future demands. Among the various kinds of nanostructures, particularly nanowires having one dimensional characteristics are the potential candidates for future nano-electronic devices.

Because, ferroelectricity and ferromagnetism (antiferromagnetism) tend to be mutually exclusive [3], only a limited multiferroic materials exist having both ferroelectricity and ferromagnetism (antiferromagnetism) simultaneously. $BiFeO_3$ is one of the mostly studied materials [4] among the limited multiferroic materials having ferroelectric curie temperature (T_C) of 830 °C and an antiferromagnetic (AFM) neel temperature (T_N) of 370 °C. In $BiFeO_3$ the weak ferromagnetism is caused by residual moment from the canted Fe^{3+} spin structure while the ferroelectricity is induced by the stereo-chemically active $6s^2$ lone pair of Bi^{3+}. The lattice distortion of $BiFeO_3$ induced the coupling between magnetic and electric behaviors, when an electric field or a magnetic field is applied [5–7]. It is reported that the magnetism and ferroelectricity in $BiFeO_3$ can be enhanced by replacing Bi site with rare-earth [8–11] or substituting Fe site with transition-metal and rare-earth [12–15].

Prasanthi et al. reported surface enhanced strong visible photoluminescence from sol–gel synthesized one-dimensional multiferroic $BiFeO_3$ nanostructures [16]. Cai et al. [17] described the ferroelectric and dielectric properties of $Bi_{3.15}Nd_{0.85}Ti_3O_{12}$ nanotubes synthesized using anodic aluminum oxide (AAO) template. Liu et al. [18] reported the spin glass transition below the freezing temperature of 55 K in $BiFeO_3$ nanowires synthesized using improved hydrothermal method. Joshi et al. [19] reported Microwave synthesis of single-crystalline perovskite $BiFeO_3$ nanocubes for photoelectrode and photocatalytic applications. Gao et al. [20] reported the synthesis of $BiFeO_3$ nanowires through AAO template. They also reported weak ferromagnetism at room temperature and superparamagnetism at low temperature in $BiFeO_3$ nanowires, different from the antiferromagnetic order in bulk $BiFeO_3$, reflecting the important size effects on the magnetic ordering of $BiFeO_3$. Jing et al. [21] reported the coexistence of ferroelectric and ferromagnetic ordering at room temperature in the $BiFeO_3$ nanotubes synthesized using sol–gel AAO template method.

The main intention of the present work is to improve the enhanced magnetic properties in $BiFeO_3$ nanowires. Appropriate magnetic ion doping may induce inter defect

S. Kumar (✉)
University College of Engineering,
Punjabi University, Patiala 147002, India
e-mail: sanjeevace_phy@yahoo.co.in

coupling [22, 23] for enhanced ferromagnetism. Gd is a promising dopant [24] for $BiFeO_3$ multiferroics system for realizing improved ferromagnetism. In the present work, we report the synthesis of Gd doped $BiFeO_3$ nanowires using sol–gel template assisted method and their structural, dielectric and magnetic properties.

2 Experimental details

Gd doped $BiFeO_3$ nanowires were synthesized by the sol–gel template assisted technique. All the reagents in the experiments were of analytic grade and used without further purification. $Fe(NO_3)_3{\cdot}9H_2O$, $Bi(NO_3)_3{\cdot}5H_2O$ and $Gd(NO_3)_2{\cdot}6H_2O$ were first dissolved in 2-methoxyethanol for 45 min by means of ultrasonic cleaner. Solution was then heated at magnetic stirrer heater at 70 °C with constant stirring for 4 h. The sols were aged for 24 h at room temperature. The commercially available anodic aluminum oxide (AAO) templates purchased from Whatman, UK, having average pore diameter, 100 nm, and pore density, 10^9 cm^{-2} have been used. AAO templates were put in the as prepared sol for 24 h. Then AAO template filled with sol were calcined at 500 °C for 1.5 h and 750 °C for 30 min.

X-Ray diffraction data was collected using a Panalytical XPERT–PRO diffractometer with Cu K_α radiation at a step of 0.02° in the range $2\theta = 20°–80°$. Scanning electron microscopic (SEM) measurements were carried out by JEOL 6100. Dielectric constant and dielectric loss were performed using an Agilent precision impedance analyzer over the frequency range from 20 to 2 MHz. For dielectric measurements, both surfaces of filled AAO template were polished with silver paste to make electrodes. Quantum design vibrating sample magnetometer (VSM) was used for the magnetic characterization of pure and Gd doped $BiFeO_3$ nanowires.

3 Results and discussion

Figure 1a depicts the XRD patterns of pure and 10 % Gd doped $BiFeO_3$ nanowires at room temperature. It is clearly evident from the XRD patterns that the structure of pure $BiFeO_3$ samples has rhombohedral symmetry, which is in agreement with the JCPDS card No. 86-1518. $BiFeO_3$ nanowires with 10 % Gd doping illustrate orthorhombic structure. Usually pure $BiFeO_3$ (x = 0) is noncentrosymmetric rhombohedral structure having space group R3c and parent $GdFeO_3$ (x = 1) is centrosymmetric orthorhombic structure having space group Pnma. Due to metastable nature of $BiFeO_3$ and its chemical kinetics of formation it is always coupled with some impurity phases as $Bi_{25}FeO_{40}$ and $Bi_2Fe_4O_9$ [25]. It is clearly depicted that (104) and (110) diffraction peaks in the vicinity of $2\theta = 32.1°$ are separated in pure $BiFeO_3$ nanowires, which get merged to a single broad (020) peak and also has a tendency to shift toward higher 2θ value when 10 % Gd ion concentration is doped in $BiFeO_3$ (Fig. 1b). Diffraction peak of (006) occurred at $2\theta = 38.85°$ has been credited as the indicator of the rhombohedral structure in pure $BiFeO_3$. This (006) peak vanishes in 10 % Gd doped $BiFeO_3$ nanowires. Disappearance of (006) peak signifies the structural phase conversion from rhombohedral to orthorhombic phase [26, 27]. One more peak indexing to (121) in the region of $2\theta = 38°–40°$ related to orthorhombic structure is observed along with disappearance of (006) and (202) peaks is also an indication of the structural conversion from its original rhombohedral structure to orthorhombic. The phase transition from rhombohedral to orthorhombic structure is ascribed to the structural deformation resulting from the inclusion of Gd^{3+} ions into the $BiFeO_3$ lattice, for the reason [28] that the ionic radius of Gd^{3+} is smaller than that of Bi^{3+}. Figure 2 shows SEM image of Gd doped $BiFeO_3$ nanowires. It is clear from Fig. 2 that the nanowires are dense and possess diameter 100 nm.

Figure 3a, b, show the frequency dependence of dielectric constant and dielectric loss in pure and 10 % Gd doped $BiFeO_3$ nanowires at room temperature, respectively. Both dielectric constant and dielectric loss decreases with increase in frequency which may be attributed due to the incapability of the electric dipoles to be in pace with the frequency of applied electric field [29, 30]. It is observed from Fig. 3a, that the values of dielectric constant were around 379 and 533 for pure and 10 % Gd doped $BiFeO_3$ nanowires, respectively at 1 kHz. Both samples show dielectric dispersion. The value of dielectric constant is high at low frequencies; it decreases quickly up to 10 kHz and shows a stable value afterwards. The observation of enhanced dielectric constant for 10 % Gd doped BiFeO3 nanowires may be due to the development of large dipole moment due to structural deformation from rhombohedral to orthorhombic.

The two sources of polarization i.e. dipolar and interfacial polarization play major role in dielectric measurement, since in the high frequency range, the value of dielectric constant becomes stable. Dipolar polarization or orientational polarization contributes to the dielectric properties in the range 10^3–10^6 Hz (sub infra-red) [31]. The interfacial polarization takes place when mobile charge carriers are obstructed by a physical barrier. As a result, the charges pile up at the barrier creates a localized polarization. Interfacial polarization occurs in the low frequency range (10^2 Hz). As pure and Gd doped $BiFeO_3$ nanowires are prepared by sol–gel template assisted technique, the complex dielectric behavior may be contributed by dipolar and interfacial polarization including localized defects. The

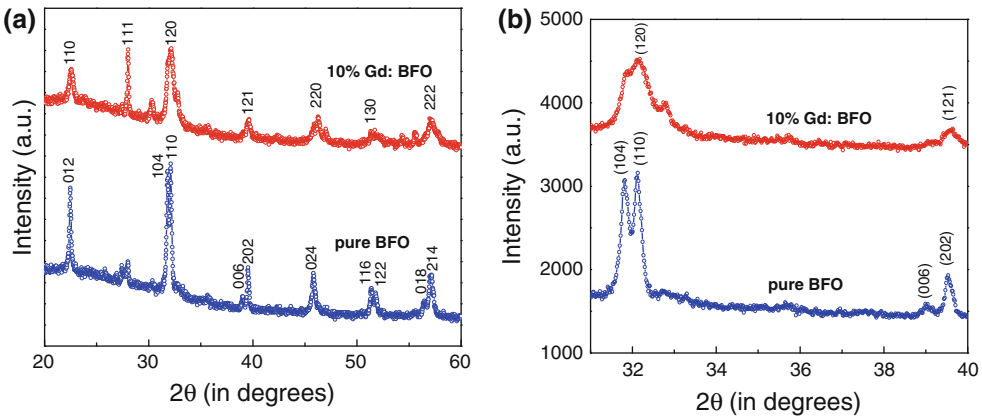

Fig. 1 **a** X-ray diffraction patterns of pure and Gd doped $BiFeO_3$ nanowires. **b** Magnified XRD patterns of pure and Gd doped $BiFeO_3$ nanowires

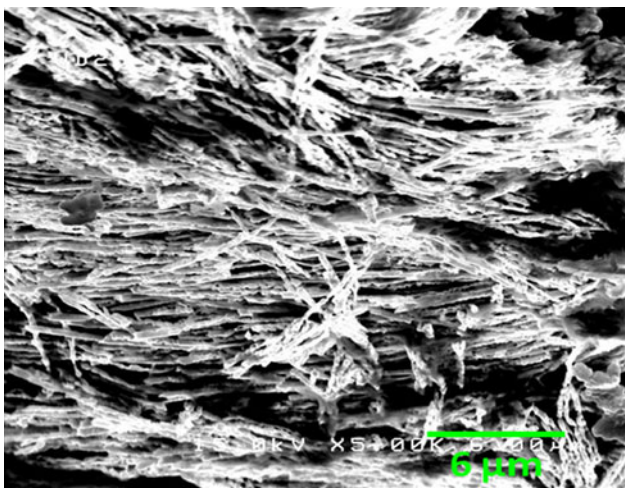

Fig. 2 SEM image of Gd doped $BiFeO_3$ nanowires

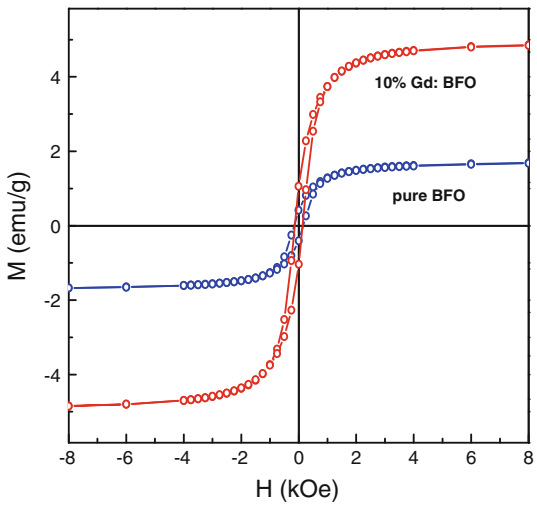

Fig. 4 M–H hysteresis curves of pure and Gd doped $BiFeO_3$ nanowires at room temperature

dielectric loss for the pure and Gd doped $BiFeO_3$ nanowires as shown in Fig. 3b, exhibit similar behaviour as observed for dielectric constant (Fig. 3a).

Magnetization versus magnetic field (M–H) loops for pure and 10 % Gd doped $BiFeO_3$ nanowires are shown in fig. 4. The M–H loops of nanowires were measured at room temperature, depicting the saturation magnetization (M_s) of pure and Gd doped $BiFeO_3$ nanowires. Different reasons may be possible for the high value of saturation magnetization and ferromagnetic character of 10 % Gd doped $BiFeO_3$ nanowires. $BiFeO_3$ exhibits distorted perovskite structure with space group R3c. Gd doping (magnetically active ions) having radius smaller than that

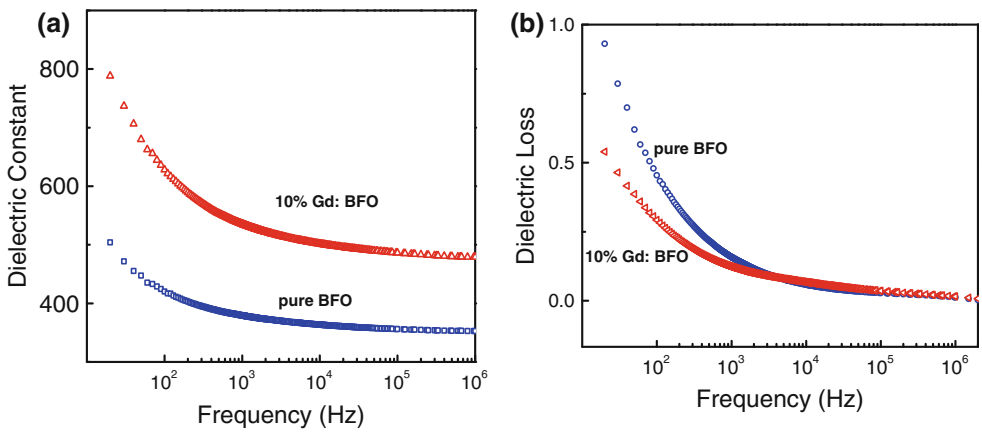

Fig. 3 **a** Variation of dielectric constant with frequency for pure and Gd doped $BiFeO_3$ nanowires at room temperature. **b** Variation of dielectric loss with frequency for Gd doped $BiFeO_3$ nanowires at room temperature

of Bi, leads to the structural distortion resulting in the destruction of spiral spin cycloid and leads to termination of the weak ferromagnetism with the release of locked magnetization [26]. The large effective magnetic moment of Gd coupled with Fe ions may be another reason for enhanced magnetization. It may also predict that more incorporation of Gd (10 %) may induce defects in the $BiFeO_3$ main matrix, which in turn stimulates defect driven ferromagnetism in Gd doped $BiFeO_3$ nanowires [32].

4 Conclusions

10 % Gd doping in $BiFeO_3$ nanowires, transforms the original rhombohedral (R3c) structure of $BiFeO_3$ into orthorhombic (Pnma) structure. Magnetic study depicts that both pure and 10 % Gd doped $BiFeO_3$ nanowires possess ferromagnetic behaviour, and saturation magnetization increases with Gd-doping. Doping of Gd also suppresses the spiral spin structure in $BiFeO_3$; as a result saturation magnetization gets enhanced. Pure and 10 % Gd doped nanowires possess frequency dependent dielectric constant, which decreases with increase in frequency and remains almost constant at higher frequencies.

Acknowledgments This work is supported by Department of Science and Technology (DST), Govt. of India under Nano Mission scheme (sanction order no. SR/NM/NS-84/2008).

References

1. W. Eerenstein, N.D. Mathur, J.F. Scott, Nature **442**, 759 (2006)
2. R. Ramesh, N.A. Spaldin, Nat. Mater. **6**, 21 (2007)
3. K.F. Wang, J.M. Liu, Z.F. Ren, Adv. Phys. **58**, 321 (2009)
4. G. Catalan, J.F. Scott, Adv. Mater. **21**, 1 (2009)
5. J. Wang, J.B. Neaton, H. Zheng, V. Nagarajan, S.B. Ogale, B. Liu, D. Viehland, V. Vaithyanathan, D.G. Schlom, U.V. Waghmare, N.A. Spaldin, K.M. Rabe, M. Wuttig, R. Ramesh, Science **299**, 1719 (2003)
6. J. Li, J. Wang, M. Wuttig, R. Ramesh, N. Wang, B. Ruette, A.P. Pyatakov, A.K. Zvezdin, D. Viehland, Appl. Phys. Lett. **84**, 5261 (2004)
7. R.R. Das, D.M. Kim, S.H. Baek, C.B. Eom, F. Zavaliche, S.Y. Yang, R. Ramesh, Y.B. Chen, X.Q. Pan, X. Ke, M.S. Rzchowski, S.K. Streiffer, Appl. Phys. Lett. **88**, 242904 (2006)
8. G.S. Lotey, N.K. Verma, J. Nanopart. Res. **14**, 742 (2012)
9. A. Gautam, K. Singh, K. Sen, R.K. Kotnala, M. Singh, Mater. Lett. **65**, 591 (2011)
10. G.D. Hu, S.H. Fan, C.H. Yang, W.B. Wu, Appl. Phys. Lett. **92**, 192905 (2008)
11. V.R. Reddy, D. Kothari, A. Gupta, S.M. Gupta, Appl. Phys. Lett. **94**, 082505 (2009)
12. M. Kumar, K.L. Yadav, J. Phys. Condens Matter **18**, L503 (2006)
13. F.G. Chang, N. Zhang, F. Yang, S.X. Wang, G.L. Song, J. Phys. D Appl. Phys. **40**, 7799 (2007)
14. M. Kumar, K.L. Yadav, J. Appl. Phys. **100**, 074111 (2006)
15. M. Azuma, H. Kanda, A.A. Belik, Y. Shimakawa, M. Takano, J. Magn. Magn. Mater. **310**, 1177 (2007)
16. K. Prashanthi, G. Thakur, T. Thundat, Surf. Sci. **606**, L83 (2012)
17. W. Cai, X. Lu, H. Bo, Y. Kan, Y. Weng, L. Zhang, X. Wu, F. Huang, L.M. Eng, J. Zhu, F. Yan, J. Appl. Phys. **110**, 052004 (2011)
18. B. Liu, B. Hu, Z. Du, Chem. Commun. **47**, 8166 (2011)
19. U.A. Joshi, J.S. Jang, P.H. Borse, J.S. Lee, Appl. Phys. Lett. **92**, 242106 (2008)
20. F. Gao, Y. Yuan, K.F. Wang, X.Y. Chen, F. Chen, J.-M. Liu, Z.F. Ren, Appl. Phys. Lett. **89**, 102506 (2006)
21. Wang Jing, Li Mei-Ya, Liu Xiao-Lian, Pei Ling, Liu Jun, Yu. Ben-Fang, Zhao Xing-Zhong, Chin. Phys. Lett. **26**, 117301 (2009)
22. V.A. Khomchenko, D.A. Kiselev, I.K. Bdikin, V.V. Shvartsman, P. Borisov, W. Kleemann, J.M. Vieira, A.L. Kholkin, Appl. Phys. Lett. **93**, 262905 (2008)
23. C.D. Pemmaraju, S. Sanvito, Phys. Rev. Lett. **94**, 217205 (2005)
24. S. Dhar, O. Brandt, M. Ramsteiner, V.F. Sapega, K.H. Ploog, Phys. Rev. Lett. **94**, 037205 (2005)
25. S.K. Pradhan, J. Das, P.P. Rout, V.R. Mohanta, S.K. Das, S. Samantray, D.R. Sahu, J.-L. Huang, S. Verma, B.K. Roul, J. Phys. Chem. Solids **71**, 1557 (2010)
26. S.K. Pradhan, B.K. Roul, J. Phys. Chem. Solids. **72**, 1180 (2011)
27. B.K. Roul, J. Supercond. **14**, 529 (2001)
28. P. Uniyal, K.L. Yadav, Mater. Lett. **62**, 2858 (2008)
29. P. Uniyal, K.L. Yadav, J. Alloys Compd. **492**, 406 (2010)
30. I. Sosnowska, T. Peterlin-Neumaier, E. Streichele, J. Phys. C: Solid State Phys. **15**, 4835 (1982)
31. S. Cavdar, H. Koralay, N. Tugluoglu, A. Gunen, Supercond. Sci. Technol. **18**, 1204 (2005)
32. S.K. Pradhan, J. Das, P.P. Rout, S.K. Das, D.K. Mishra, D.R. Sahu, A.K. Pradhan, V.V. Srinivasu, B.B. Nayak, S. Verma, B.K. Roul, J Mag. Mag. Mater. **322**, 3614 (2010)